

## THERMOELASTIC LOSSES IN STRUCTURAL MATERIALS OF WAVE SOLID-STATE GYROSCOPE RESONATORS

**B.S. Lunin, A.V. Yurin, M.A. Basarab,  
V.A. Matveev, E.A. Chumankin**

Bauman Moscow State Technical University, Moscow, Russian Federation  
e-mail: bmic@mail.ru

*One of the key features of the resonators of wave solid-state gyros is their quality factor defining in many respects the instrument's systematic and random errors. To enhance the resonator quality, it is necessary to take into consideration peculiar properties of different dissipative processes in design process. The contribution of these processes depends on the resonator material behaviour, its design, its surface processing quality, vacuum level in the instrument. Thermoelastic internal friction is a fundamental dissipative process. The influence of internal thermoelastic friction on the characteristics of resonators made of various materials is revealed by means of a thermoelastic processes model and finite-element simulation. It is shown that internal thermoelastic friction in quartz glass is very small as compared to other structural materials. It permits to recommend quartz glass as a main structural material for wave solid-state gyroscope resonators.*

**Keywords:** wave solid-state gyroscope, resonator quality factor, thermoelastic losses, finite-element simulation.

In the last decade, vibratory gyroscopes have become widespread, their operation based on Coriolis effect. The centerpieces of these instruments are mechanical resonators of various design — frame, ring, hemispherical, etc. [1, 2]. One of the main features of these resonators is their quality factor, which to a large degree determines the instrument's systematic and random errors [2]. To enhance the quality factor, materials with small thermoelastic internal friction are usually selected as structural materials: quartz glass, silicon, metals, synthetic sapphire, etc. To achieve the best results in the resonator design, one should take into consideration specific features of all dissipative processes. It will be recalled that the internal friction in a solid body is the whole set of all irreversible thermodynamic processes resulting in energy dissipation of resonator's elastic vibrations. The value of internal friction is proportional to the ratio of energy dissipated for one period of vibrations ( $\Delta W$ ), to the total resonator's energy ( $W$ ):

$$\varsigma = \Delta W / (2\pi W), \quad (1)$$

here the resonator's quality factor is  $Q = \varsigma^{-1}$ .

As the internal friction in the resonator is determined with the sum of all dissipative processes, then

$$\varsigma = \varsigma_T + \varsigma_V + \varsigma_S + \varsigma_G + \dots, \quad (2)$$

where  $\varsigma_T$  – thermoelastic internal friction;  $\varsigma_V$  – internal friction in the material structure;  $\varsigma_S$  – losses in the surface layer of the material;  $\varsigma_G$  – gas friction.

Contributions of these separate processes (their list is unbounded (2)) are different and depend on the properties of the resonator material, its design, the quality of its surface processing, the vacuum level in the instrument. The internal friction in a solid body and in its surface layer as well as gas friction are thoroughly discussed in [3–5]. The thermoelastic internal friction, depending on the properties of the material and design, can either be negligibly small or fully limit the resonator’s quality factor. The detailed calculation of thermoelastic losses permits to assess accurately enough the potential possibilities of the vibratory gyroscope design. In special literature there are examples of these calculations made for micromechanical instruments [6–8]. In wave solid-state gyroscopes (WSG), axisymmetric thin-walled shells are used as resonators and the thermoelastic losses in their material can also be significant. The objective of the present paper is to consider the influence of thermoelastic internal friction on the characteristics of WSG resonators made of various materials.

**Simulation of thermoelastic internal friction in a resonator.** Physics of thermoelastic internal friction was first revealed by Zener [9] who associated it with the onset of heat flows under deformation of a solid body. In resonator’s vibrations, the deformations of its parts are opposite in sign, i.e. in some places the material expands and in other places it contracts. The body volume change under deformation requires that some work  $A$  should be done, which can be expressed through thermal expansion coefficient ( $\alpha$ ) and modulus of elasticity ( $E$ ) [10] as follows:

$$A = 9\alpha^2 TEV, \quad (3)$$

where  $T$  – body temperature;  $V$  – molar volume of the substance.

It follows from (3) that when a solid body is under deformation (if  $\alpha \neq 0$ ), the temperature in different parts of the body will depend on deformation. In its turn, the inequality of these temperatures will result in the onset of local heat flows increasing the oscillator’s entropy, which is equivalent to the irreversible transformation of mechanical energy into heat energy. To assess the thermoelastic losses quantitatively, Zener suggested simple formulas that provide good enough compliance with the experiment in relation to a range of metals within the bounds of his phenomenological model of internal friction in a solid body.

In the present paper, to determine thermoelastic losses, the finite-element simulation of thermoelastic damping according to the second mode shape in a cylindrical resonator was used (Fig. 1, *b, c*).

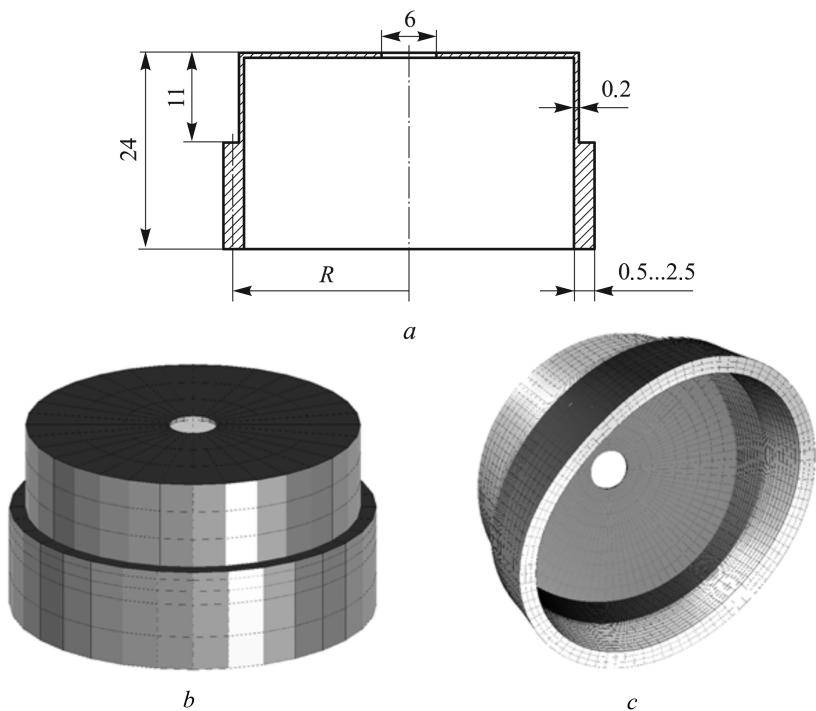


**Fig. 1.** Design drawing of WSG resonator (a), finite-element approximation of geometry (b) and its deformation according to the second mode shape (c)

This structure (as well as the simulated mode shape) is of a certain practical interest because it is used in a number of modern developments [11, 12]. The temperature field along the circular angle, heat flows and the loss of resonator's energy for one period were calculated for a specified deformation of the cylindrical shells subject to the properties of its material. The characteristics of materials used in simulation are given in the table below. The geometry of WSG resonator are given in Fig. 1, a.

The thickness of the resonator working area  $b$  and the central radius of the working area  $R$  exert the main influence upon the change of resonator's characteristic features. The other dimensions do not exert significant influence upon the result. In simulating,  $b$  takes on values 0.5, 1.0, 1.5, 2.0 and 2.5 mm, while  $R$  changes in a wide range.

The finite-element formulation of the task is based on the approximate method of solving interconnected tasks of the dynamic theory of elasticity and nonpermanent thermal conductivity [13]. According to the theory of thermoelasticity, the connection between vectors of stresses and deformations is set in the form

$$\boldsymbol{\sigma} = \mathbf{D}\boldsymbol{\varepsilon} = \mathbf{D}(\boldsymbol{\varepsilon}_{EL} - \boldsymbol{\varepsilon}_T), \quad (4)$$

where  $\boldsymbol{\varepsilon}_{EL}$ ,  $\boldsymbol{\varepsilon}_T$  – tensors of elastic and temperature deformations;  $\boldsymbol{\sigma}$  – stress tensor;  $\mathbf{D}$  –  $6 \times 6$  elastic constant tensor.

### Physical parameters of materials

Material parameters	Material				
	Aluminum (Д16Т)	Steel (12Х18Н10Т)	Silicon (Si)	Sapphire (Al <sub>2</sub> O <sub>3</sub> )	Quartz (SiO <sub>2</sub> )
Density, $\rho$ , kg/m <sup>3</sup>	2800	7900	2320	3980	2220
Poisson's ratio, $\nu$	0.33	0.30	0.28	0.25	0.18
Young's modulus, $E$ , Па	$7.08 \cdot 10^{10}$	$1.98 \cdot 10^{11}$	$1.30 \cdot 10^{11}$	$4.40 \cdot 10^{11}$	$7.20 \cdot 10^{10}$
Heat expansion rate, $\alpha$ , 1/°C	$2.30 \cdot 10^{-5}$	$1.66 \cdot 10^{-5}$	$4.20 \cdot 10^{-6}$	$6.60 \cdot 10^{-6}$	$6.00 \cdot 10^{-7}$
Specific heat, $C_p$ , J/kg·°C	922	462	1414	790	728
Volumetric heat capacity, $C_V$ , J/m <sup>3</sup> ·°C	$2.58 \cdot 10^{-6}$	$3,65 \cdot 10^{-6}$	$3.28 \cdot 10^{-6}$	$3.14 \cdot 10^{-6}$	$1.62 \cdot 10^{-6}$
Heat conductivity coefficient, $k$ , W/(m·°C)	237	15	150	40	1,35

Stress tensors and deformation tensors consist of  $x$ ,  $y$  and  $z$  normal components and  $x$ - $y$ ,  $y$ - $z$  и  $z$ - $x$  tangent components.

The equations of elastic medium motion are obtained if the force of internal stresses  $\nabla \cdot \boldsymbol{\sigma}$  is equated to the product of acceleration and mass of a solid body volume unit (i.e. its density)  $\rho \ddot{\mathbf{u}}$ . The vector form of the motion equation is

$$\rho \frac{\partial^2 \mathbf{u}}{\partial t^2} = \nabla \cdot \boldsymbol{\sigma}. \quad (5)$$

Here  $\rho$  – volume density;  $\mathbf{u}$  – displacement vector.

Equations (4) and (5) form a total system of differential equations in partial derivatives for stresses and deformations. Boundary conditions should be added to (4) и (5), but we will not dwell on them.

The connection of deformation with temperature is set using thermodynamics laws. The equation of thermal conductivity at a small thermal disturbance (i.e. with  $(T - T_0)/T_0 \ll 1$ ) can be written as

$$C_V \frac{\partial T}{\partial t} - \nabla(k \nabla T) = \dot{q}, \quad (6)$$

where  $C_V = \rho C_p$  – volumetric heat capacity;  $C_p$  – specific heat;  $k(\chi)$  – heat conductivity coefficient;  $\dot{q}$  – heat source, namely, heat generation rate in the unit of volume.

In case of thermoelastic heating, the heat source for an isotropic material is determined as follows:

$$\dot{q} = - \frac{E \alpha T_0}{(1 - 2\nu)} \frac{\partial e}{\partial t}, \quad (7)$$

where  $E$  – Young’s modulus;  $\alpha$  – heat conductivity coefficient;  $T_0$  – temperature of the environment (initial temperature);  $e$  – expansion deformation;  $\nu$  – Poisson’s ratio.

For  $e$ , the following relation is true

$$e = \varepsilon_x + \varepsilon_y + \varepsilon_z = \nabla \cdot \mathbf{u}. \quad (8)$$

Let us try to look for a solution of equation for  $\Delta T$  and  $\mathbf{U}$  in the form

$$\begin{aligned} \Delta T &= T - T_0 = e^{\lambda t} \Theta, \\ \mathbf{u} &= e^{\lambda t} \mathbf{U}, \\ \mathbf{v} = \dot{\mathbf{u}} &= e^{\lambda t} \mathbf{V}, \end{aligned} \quad (9)$$

where  $\lambda = i\omega + \delta$ .

It should be noted that  $\Theta$ ,  $\mathbf{U}$ ,  $\mathbf{V}$  depend on coordinates and the number of vibrations tone  $n$  only. In simulating, only the second mode shape was considered (Fig. 1,  $c$ ).

Using Galerkin’s standard scheme/pattern for the finite element method [14] we obtain from (6)–(8) a matrix equation for temperature  $\Theta$  and displacements  $\mathbf{U}$  in mesh points:

$$(\mathbf{K} + \lambda \mathbf{H})\Theta + \lambda \mathbf{F}\mathbf{U} = 0; \quad (10)$$

here  $\mathbf{K}$ ,  $\mathbf{H}$ ,  $\mathbf{F}$  – matrices whose elements are composed from shape functions  $\mathbf{N}$  with number of mesh points  $m$ .

The axisymmetric resonator’s geometry assumes the transition to cylindrical coordinates  $r$ ,  $\theta$ ,  $z$ . Then (6) will take on the form

$$\rho C_P \frac{\partial T}{\partial t} - k \left( \frac{\partial^2 T}{\partial r^2} + \frac{1}{r} \frac{\partial T}{\partial r} + \frac{1}{r^2} \frac{\partial^2 T}{\partial \theta^2} + \frac{\partial^2 T}{\partial z^2} \right) = - \frac{E\alpha T_0}{(1 - 2\nu)} \frac{\partial e}{\partial t},$$

while for element matrices from (10) the following relations are true:

$$\mathbf{K}_e = \int_{\Omega} k \left( \frac{\partial \mathbf{N}}{\partial r} \frac{\partial \mathbf{N}^T}{\partial r} + \frac{\partial \mathbf{N}}{\partial z} \frac{\partial \mathbf{N}^T}{\partial z} + \frac{n^2}{r^2} \mathbf{N} \mathbf{N}^T \right) dr dz,$$

$$\mathbf{H}_e = \int_{\Omega} C_V \mathbf{N} \mathbf{N}^T dr dz,$$

$$\mathbf{F} = [\mathbf{F}_1 \dots \mathbf{F}_m],$$

$$\mathbf{F}_i = \frac{E\alpha T_0}{1 - 2\nu} \mathbf{N} \begin{bmatrix} \frac{\partial \mathbf{N}_i}{\partial r} + \frac{\mathbf{N}_i}{r} - \frac{n\mathbf{N}_i}{2r} + \frac{1}{2} \frac{\partial \mathbf{N}_i}{\partial z} \\ \frac{n\mathbf{N}_i}{r} + \frac{1}{2} \left( \frac{\partial \mathbf{N}_i}{\partial r} - \frac{\mathbf{N}_i}{r} \right) + \frac{1}{2} \frac{\partial \mathbf{N}_i}{\partial z} \\ \frac{\partial \mathbf{N}_i}{\partial z} - \frac{n\mathbf{N}_i}{2r} + \frac{1}{2} \frac{\partial \mathbf{N}_i}{\partial z} \end{bmatrix}^T, \quad (i = 1, \dots, m).$$

Equation of motion (5) when using (4), (8) in matrix form

$$\boldsymbol{\sigma} = \mathbf{C}\boldsymbol{\varepsilon} - \mathbf{D}\mathbf{T},$$

$$\boldsymbol{\varepsilon} = \mathbf{B}\mathbf{U},$$

Can be transformed into the following form:

$$\mathbf{L}\mathbf{U} - \mathbf{G}\boldsymbol{\Theta} + \boldsymbol{\lambda}\mathbf{M}\mathbf{V} = 0. \quad (11)$$

Here  $\mathbf{L}$ ,  $\mathbf{G}$ ,  $\mathbf{M}$  – element matrices, and  $\mathbf{V}$  – vector of rate values at mesh points.

Elements of matrices in (8)–(11) are calculated in the following way:

$$\mathbf{L}_e = \int_{\Omega} \mathbf{B}^T \mathbf{C} \mathbf{B} \, dr \, dz, \quad \mathbf{G}_e = \int_{\Omega} \mathbf{B}^T \mathbf{D} \mathbf{B} \, dr \, dz, \quad \mathbf{M}_e = \int_{\Omega} \rho \mathbf{N} \mathbf{N}^T \, dr \, dz.$$

Matrices  $\mathbf{C}$ ,  $\mathbf{D}$ ,  $\mathbf{B}$  depend on physical properties of the material and the form of interpolation functions

$$\mathbf{C} = \frac{E}{(1 + \nu)(1 - 2\nu)} \begin{bmatrix} 1 - \nu & \nu & \nu & 0 & 0 & 0 \\ \nu & 1 - \nu & \nu & 0 & 0 & 0 \\ \nu & \nu & 1 - \nu & 0 & 0 & 0 \\ 0 & 0 & 0 & 1/2 - \nu & 0 & 0 \\ 0 & 0 & 0 & 0 & 1/2 - \nu & 0 \\ 0 & 0 & 0 & 0 & 0 & 1/2 - \nu \end{bmatrix},$$

$$\mathbf{D} = \frac{E\alpha}{(1 - 2\nu)} [1 \ 1 \ 1 \ 0 \ 0 \ 0]^T,$$

$$\mathbf{B} = [\mathbf{B}_1 \ \dots \ \mathbf{B}_m],$$

$$\mathbf{B}_i = \begin{bmatrix} \frac{\partial \mathbf{N}_i}{\partial r} & 0 & 0 \\ \frac{\mathbf{N}_i}{r} & \frac{n\mathbf{N}_i}{r} & 0 \\ 0 & 0 & \frac{\partial \mathbf{N}_i}{\partial z} \\ -\frac{n\mathbf{N}_i}{2r} & \frac{1}{2} \left( \frac{\partial \mathbf{N}_i}{\partial r} - \frac{\mathbf{N}_i}{r} \right) & 0 \\ 0 & \frac{1}{2} \frac{\partial \mathbf{N}_i}{\partial z} & \frac{n\mathbf{N}_i}{2r} \\ \frac{1}{2} \frac{\partial \mathbf{N}_i}{\partial z} & 0 & \frac{1}{2} \frac{\partial \mathbf{N}_i}{\partial r} \end{bmatrix}, \quad (i = 1, \dots, m).$$

Basing on the fact that the connection between displacements and the rates at mesh points is set by relation [13]

$$\mathbf{V} = \lambda \mathbf{U}, \quad (12)$$

and also using (10) and (11), we obtain the equation for the calculation of  $\lambda$  eigenvalues

$$\begin{bmatrix} -\mathbf{K} & 0 & 0 \\ \mathbf{G} & -\mathbf{L} & 0 \\ 0 & 0 & \mathbf{I} \end{bmatrix} \begin{bmatrix} \Theta \\ \mathbf{U} \\ \mathbf{V} \end{bmatrix} = \lambda \begin{bmatrix} \mathbf{H} & \mathbf{F} & 0 \\ 0 & 0 & \mathbf{M} \\ 0 & \mathbf{I} & 0 \end{bmatrix} \begin{bmatrix} \Theta \\ \mathbf{U} \\ \mathbf{V} \end{bmatrix}, \quad (13)$$

where  $\mathbf{I}$  is a unit matrix.

The eigenvalue is complex value  $\lambda = \delta + j\omega$  that explicitly determines resonance vibration frequency  $\omega$  and damping coefficient  $\delta$ .

Let us write the relation for obtaining resonator's quality factor  $Q$  on resonance frequency  $f$  in the following form:

$$Q = \frac{\text{Im}(\lambda)}{2 \text{Re}(\lambda)}, \quad \delta = \text{Re}(\lambda), \quad f = \left| \frac{\text{Im}(\lambda)}{2\pi} \right|. \quad (14)$$

In addition, to every  $\lambda_n$  eigenvalue, there corresponds its own harmonic field of a heat flow, displacements, stresses and deformations. As the intensities of heat flows depend on both the thickness of resonator's wall ( $b$ ), and vibration frequency ( $f$ ), the results of the calculation for various structural materials are shown in Fig. 2, 3 in the form of dependencies  $Q(f, b)$ . Here, it was supposed that  $Q = \zeta_T^{-1}$ , while the intensities of all other dissipative processes mentioned in (2), were equal to zero.

**Results and discussion.** In Fig. 2 the data is shown on the quality factors of metal resonators made of duraluminium Д16Т and corrosion-resistant steel. As one can see in the picture, the quality factor of thin-walled (less than 1 mm) and low-frequency (less than 1 kHz) metal resonators is always small (about 1000) because of high intensity of the thermoelastic internal friction, which is also a dominating dissipative process. To get the quality factor  $(4 \dots 5) \cdot 10^4$ , the wall thickness should be taken equal to not less than 1 ... 1.5 mm, while the working frequency should be not less than 4 ... 5 kHz.

Rather small values of resonators' quality factor can be received using silicon and sapphire as structural materials (Fig. 3). At the vibration frequency up to 10 kHz of these resonators, thermoelastic losses will limit their quality factor on the level  $10^6$ . In contrast to these materials, quartz glass has a low level of thermoelastic internal friction. At the vibration frequency about 1 kHz, even for wall thickness 0.5 mm, the quality factor

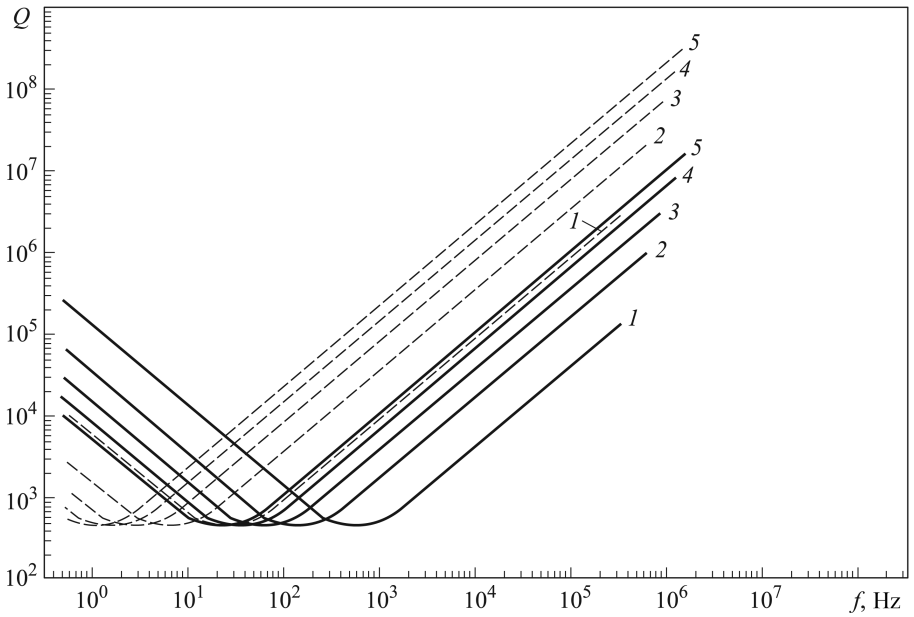


**Fig. 2. Dependence of quality factor  $Q$  on frequency  $f$  at fixed resonator's wall thicknesses for duraluminium Д16Т and corrosion-resistant steel 36НХТЮ; wall thickness  $b$ :**

1 – 0.5 mm, 2 – 1.0 mm, 3 – 1.5 mm, 4 – 2.0 mm, 5 – 2.5 mm

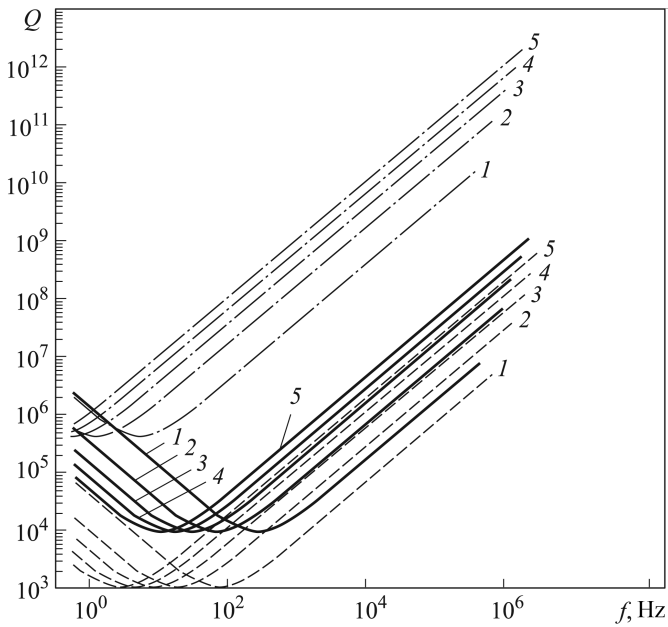


**Fig. 3. Dependence of quality factor  $Q$  on frequency  $f$  at fixed resonator's wall thicknesses for silicon, sapphire and quartz; wall thickness  $b$ :**

1 – 0.5 mm, 2 – 1.0 mm, 3 – 1.5 mm, 4 – 2.0 mm, 5 – 2.5 mm



is limited with value  $10^7$ . At higher vibration frequencies, this type of internal friction in quartz glass can be neglected.

**Conclusion.** Thermoelastic internal friction is a fundamental dissipative process whose intensity in thin-walled mechanical resonators can be high. In kHz range of frequencies, with WSG resonator wall thicknesses equal to 0.5...1.0 mm, this type of internal friction limits the quality factor of resonators made of corrosion-resistant steel and aluminium alloys on the level of some tens of thousands, while the quality factor of resonators made of silicon and sapphire is limited on the level of  $10^5$ . In quartz glass, the thermoelastic internal friction is very small, which permits to recommend it as the basic structural material for WSG resonators.

## REFERENCES

- [1] Raspopov V.Ya. Mikromekhanicheskie pribory [Micromechanical instruments]. Moscow, Mashinostroenie Publ., 2007. 400 p.
- [2] Loper E.J., Lynch D.D., Stevenson K.M. Projected performance of smaller hemispherical resonator gyros // *Proc. Position Location and Navigation Symposium (PLANS'86)*. 1986, November 4–7. Las Vegas, NV, USA, pp. 61–64.
- [3] Postnikov V.S. Vnutrennee trenie v metallakh [Internal friction in metals]. Moscow, Metallurgiya Publ., 1968. 330 p.
- [4] Braginsky V.B., Mitrofanov V.P., Panov V.I. Sistemy s maloy dissipatsiyey [Systems with small dissipation]. Moscow, Nauka Publ., 1981. 142 p.
- [5] Lunin B.S. Fiziko-khimicheskie osnovy razrabotki polusfericheskikh rezonatorov volnovykh tverdotelnykh giroskopov [Physical and chemical theories for the development of hemispherical resonator gyroscopes]. Moscow, MAI Publ., 2005, 224 p.
- [6] Yi Y.B. Geometric effects on thermoelastic damping in MEMS resonators. *Journal of Sound and Vibration*, 2008, vol. 309, pp. 588–599.
- [7] Wong S.J., Fox C.H.J., McWilliam S. Thermoelastic damping of the in-plane vibration of thin silicon rings. *Journal of Sound and Vibration*, 2006, vol. 293, pp. 266–285.
- [8] Prabhakar S., Vengallatore S. Thermoelastic damping in bilayered micromechanical beam resonators. *Journal of Micromechanics and Microengineering*, 2007, vol. 17, pp. 532–538.
- [9] Zener C.M. Elasticity and Anelasticity of Metals. USA, Chicago, Univ. of Chicago Press, 1948 (Russ. ed.: Ziner K. Uprugost' i neuprugost' metallov [Elasticity and Anelasticity of Metals], S.V. Vonsovskiy ed. Moscow, Inostrannaya Lit. Publ., 1954. 248 p.).
- [10] Kikoin A.K., Kikoin I.K. Kurs obshchey fiziki. Molekulyarnaya fizika [General physics course. Molecular Physics]. Moscow, Nauka Publ., 1976. 480 p.
- [11] Chikovani V.V., Yatsenko Yu.A. Investigation of azimuth accuracy measurement with metallic resonator Coriolis vibratory gyroscope. *Proc. XVII Int. Conf. on Integrated Navigation Systems*. St. Petersburg, 2010, May 31–June 2, pp. 25–30.
- [12] Sarapuloff S.A., Lytvinov L.A., Bakalor T.O. Particularities of designs and fabrication technology of high-Q sapphire resonators of CRG-1 type solid-state gyroscopes. *Proc. XIV Int. Conf. on Integrated Navigation Systems*. St. Petersburg, 2007, May 28–30, pp. 47–48.
- [13] Yi Y.B. Finite element analysis of thermoelastic damping in contour-mode vibrations of micro- and nanoscale ring, disk and elliptical plate resonators// *Journal of Vibration and Acoustics*, 2010, vol. 132.

[14] Mitchell A.R., Wait R. The Finite Element Method in Partial Differential Equations. London–New York–Sydney–Toronto, John Wiley & Sons, 1977.

The original manuscript was received by the editors of “Vestnik” on 02.12.2014

## Contributors

Lunin B.S. — Dr. Sci. (Eng.), leading researcher of Chemistry department of Lomonosov Moscow State University. Author of a number of research publications in the field of vibratory gyroscope technology.

Lomonosov Moscow State University, Leninskie Gory, 1, Moscow, 119991 Russian Federation.

Yurin A.V. — programmer in the Scientific and Educational Complex for Information Technologies and Control Systems of Bauman Moscow State Technical University. Author of 15 publications in the field of mathematical modelling and digital signal processing.

Bauman Moscow State Technical University, 2-ya Baumanskaya ul., 5, Moscow, 105005 Russian Federation.

Basarab M.A. — Dr. Sci. (Phys.-Math.), professor of “Information Security” department of Bauman Moscow State Technical University. Author of 5 monographs and over 100 publications in the fields of applied mathematics, informatics, digital signal processing, and radiophysics.

Bauman Moscow State Technical University, 2-ya Baumanskaya ul., 5, Moscow, 105005 Russian Federation.

Matveev V.A. — Dr. Sci. (Eng.), professor, Head of “Information Security” department of Bauman Moscow State Technical University, Head of the Scientific and Educational Complex for Information and Control of Bauman Moscow State Technical University. Author of over 200 publications and 25 patents in the field of instrument engineering and high-temperature superconductivity.

Bauman Moscow State Technical University, 2-ya Baumanskaya ul., 5, Moscow, 105005 Russian Federation.

Chumankin E.A. — Cand. Sci. (Eng.), deputy head of the department of the public corporation “Arzamasskoe nauchno-proizvodstvennoe predpriyatie (ANPP) [Arzamas scientific production enterprise (ASPE)] “TEMP-AVIA”. Expert in the field of gyroscopic systems and navigation instruments.

Public corporation “ASPE “TEMP-AVIA”, ul. Kirova 26, Arzamas, Nizhny Novgorod region, 607920 Russian Federation.

*The translation of this article from Russian into English is done by O.G. Rumyantseva, senior lecturer, Linguistics Department, Bauman Moscow State Technical University under the general editorship of N.N. Nikolaeva, Ph.D. (Philol.), Associate Professor, Linguistics Department, Bauman Moscow State Technical University.*